

# The gellan sol–gel transition

M. Milas & M. Rinaudo

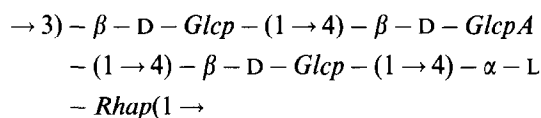
Centre de Recherches sur les Macromolécules Végétales, CERMAV-CNRS, BP 53, 38041 Grenoble, cedex 9, France,  
 affiliated with the Joseph Fourier University of Grenoble

The behavior of gellan during the conformational transition is discussed. This transition corresponds to the formation of a double helix from two separate coils. The influence of the counterion activity on the melting and gelling temperatures of the gels and/or the ordered conformation is also described.

The sol–gel transition is studied by conductimetry in the presence of pure monovalent counterions or monovalent divalent mixtures. This method is one of the best ways of characterizing this transition. A two-step mechanism of gelation was demonstrated in the presence of monovalent counterions. In the presence of divalent counterions, at a given ionic strength, the mechanism of gelation and the gel properties depend only on the ratio  $Y$  between divalent and monovalent counterions. Three types of gel behavior are described as a function of  $Y$  and ionic strength. Copyright © 1996 Elsevier Science Ltd

## INTRODUCTION

Gellan is a bacterial polysaccharide produced by *Pseudomonas elodea*; it is well known that native gellan forms a soft gel, but after alkaline hydrolysis of the side groups, it forms rigid and clear gels which are in some respects comparable with agarose; gellan is a linear polymer whose chemical structure was proposed by (Jansson *et al.*, 1983).



This structure is that of commercial gellan, produced by Kelco (USA) under the trade name Gelrite.

This paper will summarize our work on the characterization of gellan in solution, on its main properties, on the mechanism of gelation and on the gel properties.

## MATERIALS AND METHODS

### Materials

The deacetylated gellan (Gelrite) was purified following the procedure previously described (Milas *et al.*, 1990). The different ionic forms of gellan were obtained directly during the purification procedure. The solutions were prepared by dissolving the powder in water, then, solutions of salts were added in order to obtain the desired salt concentration. The gels are obtained following the same procedure but the salts were added at 90°C, and the solutions were poured into a cylindrical

mould (diameter = 17mm). After 24h at room temperature, the gels were formed and cut into small cylinders (height = 17mm). The gel volumes have been determined by weighing, assuming a density of 1.

### Methods

The conductance, potentiometric and optical rotation measurements were described previously (Milas *et al.*, 1990). The n.m.r. spectra were recorded on an AC 300 Bruker spectrometer equipped with a process controller, an ASPECT 3000 computer and a variable temperature system. The mechanical properties of gels were obtained by compression between parallel plates with an Instron 4301 instrument, at a constant deformation rate (25mm/min<sup>-1</sup>) and at room temperature. The elastic moduli were calculated from the linear region of the stress strain diagram (length of deformation < 1mm).

## CHARACTERIZATION AND SOLUTION PROPERTIES

The properties of gellan were investigated on purified samples, in order to eliminate the divalent counterions, and to obtain the samples under a single type of counterion. Gellan is a polyelectrolyte and the activity of counterions is directly related to the charge parameter  $\lambda$ :

$$\lambda = \frac{ve^2}{DhkT} \sim 1/b$$

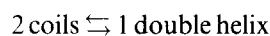
with  $v/h$  = the number of charge  $v$  on a chain of length  $h$ , and  $b$  the distance between two charged groups. Determi-

nation of the activity of counterions gives information on the conformation of the polymer in dilute solutions, in particular to determine if the polymer adopts a single or double helical structure.

In dilute solution, a reversible conformational transition ( $T_m$ ) is monitored by increasing the temperature; optical rotation and n.m.r. show a steep transition (Figs 1 and 2). These results also show that when  $D_2O$  is used as solvent for  $^1H$  n.m.r.  $T_m$  is displaced to a higher temperature ( $+6^\circ C$ ), indicating the role of hydrogen bonds and water molecules involved in the helical structure (Fig. 2). The  $^1H$  n.m.r. spectrum of gellan over the melting temperature is given in Fig. 3. (Shi, 1990).

On both sides of the conformational transition, the coefficient of transport ( $f$ ) of counterions ( $Na^+$  and  $Ca^{2+}$ ) was determined and compared with the values

calculated by the Manning theory. We have discussed this point previously (Milas *et al.*, 1990), and shown that the experimental data implies a conformational transition:



with charge parameters  $\lambda_c = 0.37$  and  $\lambda_h = 0.75$ , respectively. These results agree with those previously obtained (Grasdalen & Smidsrod, 1987; Crescenzi *et al.*, 1987).

The helical conformation stabilized in solution, which fits very well with the parameters given by Chandrasekaran which established the structure of gellan in the solid state (Chandrasekaran *et al.*, 1988; Chandrasekaran & Thailambal, 1990).

The weight average molecular weight of gellan was also determined on both sides of the transition in conditions for which there is no aggregation i.e. on the

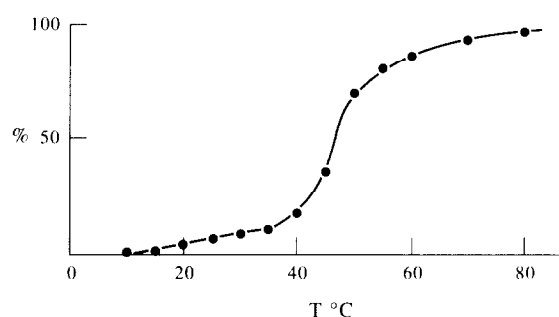


**Fig. 1.** Percentage of the methyl groups of the rhamnose unit observed by  $^1H$  n.m.r. in  $D_2O$  as a function of temperature. Na-gellan 4g/l. Calibration with sodium succinate ( $6.5 \times 10^{-2} M$ ) used as standard. 100% refers to the methyl groups of rhamnose present in the solution.

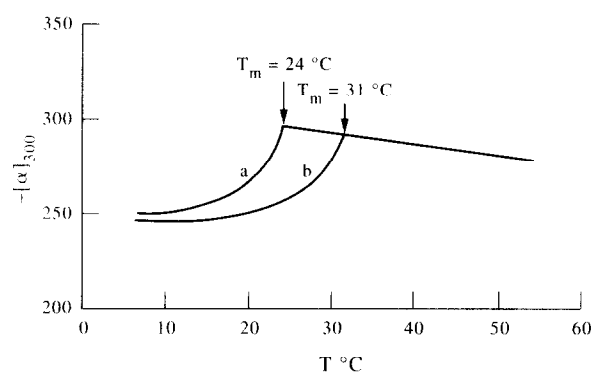


**Fig. 2.** Specific optical rotation at 300nm as a function of temperature in (a)  $H_2O$  and (b)  $D_2O$ . Na-gellan 6g/l.

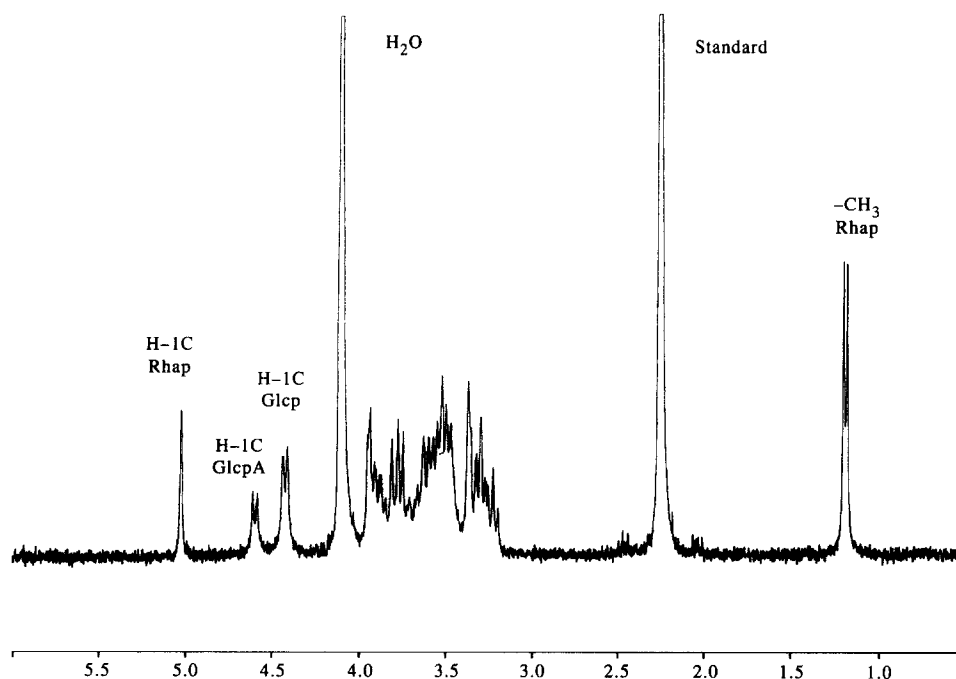


**Fig. 3.**  $^1H$  n.m.r. spectrum of Na-gellan (4g/l) in  $D_2O$  at  $80^\circ C$ .

**Table 1.** Average molecular weight,  $M_w$ , intrinsic viscosity,  $[\eta]$ , radius of gyration,  $R_G$  and intrinsic persistence length,  $L_p$  of TMA-gellan in 0.025M TMACl in the ordered ( $T = 24^\circ\text{C}$ ) and disordered conformation ( $T = 36^\circ\text{C}$ )

	Ordered conformation	Disordered conformation
$M_w$	$4.9 \times 10^5$	$2.5 \times 10^5$
$[\eta]$ (ml/g)	3 500	580
$R_G$ (Å)	1 270	695
$L_p$ (Å)	720	60

TMA salt form. The dimensions of the molecule also depend on the conformation, and was related to the intrinsic persistence length ( $L_p$ ) of the molecules; the results are summarized in Table 1.

In dilute solution, divalent counterions are much more effective for inducing the conformational change and gives a hysteresis, even in the absence of external salt; for the conditions given in Fig. 4, the ionic concentration is very low i.e.  $[\text{Mg}^{2+}] \sim 6 \times 10^{-4}$  equiv/l.

The thermal stability of the helical conformation, directly reflected by the values of  $T_m$ , depends on the total activity of the counterions for monovalent and divalent counterions. The dependence of  $T_m$  is given on Fig. 5.

It is established that the enthalpy of conformational change is given by:

$$\Delta H = -R(\phi_c - \phi_h) d \ln C_T / d(1/T_m)$$

with  $\phi$  the osmotic coefficient of the counterions under the coil and helical conformation (corresponding to  $\lambda_c = 0.37$  and  $\lambda_h = 0.75$ ).

The slopes  $d \ln C_T / d(1/T_m)$  are equal to  $-10610$  and  $-16120$  for monovalent and divalent counterions, respectively, and allow the enthalpy of the conformational change to be calculated (Table 2).

The calculated values are nearly twice that determined experimentally ( $\Delta H$  in the absence of a gel in the Na form is around 7KJ/mol) (Robinson *et al.*, 1988). This may be related to the values of  $\phi$ , which are calculated for infinite dilution in the absence of any aggregation.

## GELATION IN THE PRESENCE OF MONOVALENT COUNTERIONS

Above a critical ionic concentration  $C_T^*$ , depending on the counterions when  $\text{K}^+$  is compared with  $\text{Na}^+$ , an hysteresis exists between the position of the conformational change associated with the sol-gel transition, determined from cooling and heating curves (Fig. 6):

$$C_T(\text{K}^+) = 2 \times 10^{-2} \text{equiv/l}$$

$$C_T(\text{Na}^+) = 4.5 \times 10^{-2} \text{equiv/l}$$

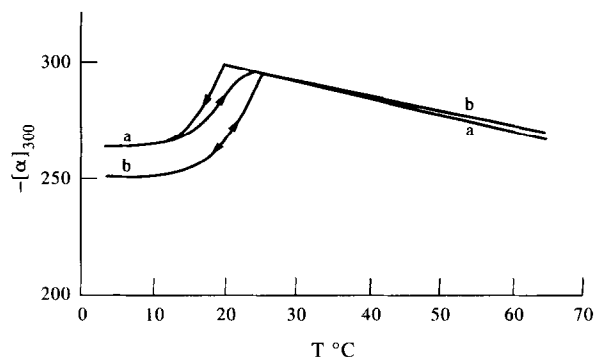


**Fig. 4.** Specific optical rotation at 300nm as a function of temperature in salt free solution. (a) Mg-gellan 0.5g/l, (b) TMA-gellan (5g/l) on cooling and heating.

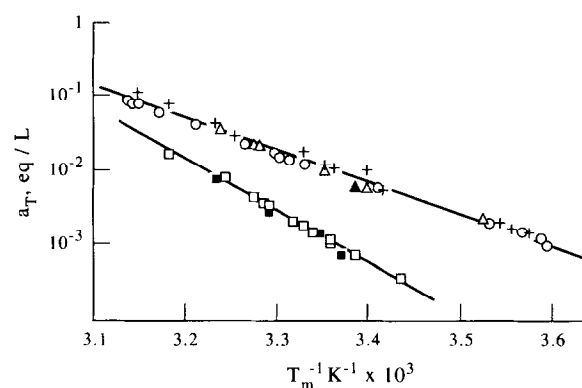


**Fig. 5.** Dependence of the inverse of the temperature of conformational transition ( $T_m^{-1}$ ) as a function of the activity of counterions. + Na-gellan, NaCl; O K-gellan, KCl; Δ TMA-gellan, TMACl; ▲ Li-gellan, LiCl; □ Ca-gellan, CaCl<sub>2</sub>; ■ Mg-gellan, MgCl<sub>2</sub> (values are determined on cooling curves).

**Table 2.** Charge parameter  $\lambda$ , osmotic coefficients for monovalent ( $\phi^+$ ) and divalent ( $\phi^{2+}$ ) counterions in the coil and helix gellan conformation. Enthalpy of conformational change,  $\Delta H$  in the presence of (a) monovalent counterions and (b) divalent counterions

	$\lambda$	$\phi^+$	$\phi^{2+}$
Coil	0.37	0.815	0.407
Helix	0.75	0.625	0.312
$\Delta H$		(a) 16KJ/mol	(b) 12.7KJ/mol

This behavior is similar to that found for K-carrageenan, where the corresponding values were:

$$C_T(\text{K}^+) = 7 \times 10^{-3} \text{equiv/l}$$

$$C_T(\text{Na}^+) = 2 \times 10^{-1} \text{equiv/l}$$

It is also important to point out that for gellan there is no selectivity between the monovalent counterions under  $C_T^*$  in relation to its low charge parameter, when compared to K-carrageenan for which ionic selectivity exists even in the coil conformation (Rinaudo *et al.*, 1983).

Conductivity of a gellan solution was tested as a

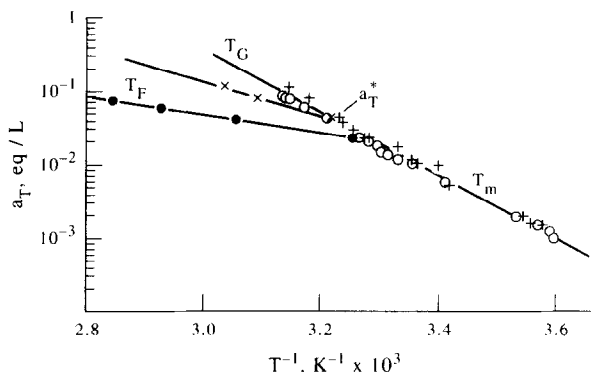


**Fig. 6.** Phase diagram for gellan in the presence of monovalent counterions when  $\log$  (total activity of counterions) is plotted as a function of the inverse of the temperature of transition:  $T_m$  the conformational temperature change (coil  $\rightarrow$  helix), superposes with the sol-gel transition ( $T_G$ ) over a critical  $a_T^*$  on cooling;  $T_F$  is the melting temperature of the gel. Na-gellan: (x) heating (+) cooling (●) K-gellan: (●) heating (○) cooling

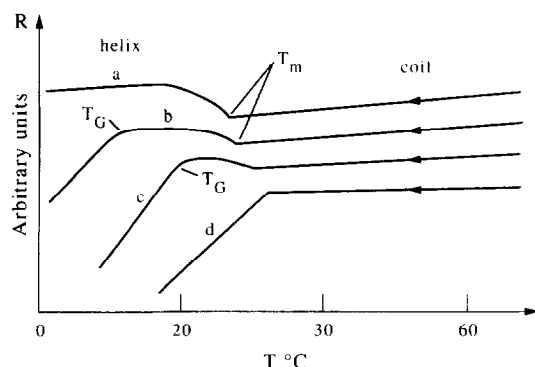


**Fig. 7.** Influence of the temperature on the specific conductivity of K-gellan expressed by the ratio  $R$  (see text). K-gellan 10g/l in (a) water, (b)  $2 \times 10^{-3}$  N KCl, (c)  $6 \times 10^{-3}$  N KCl, (d)  $1 \times 10^{-2}$  N KCl. The curves are obtained on cooling.

function of temperature, and compared with that of a simple electrolyte solution having the same specific conductivity at 25°C. The ratio of these two values ( $R$ ) is plotted as a function of temperature in Fig. 7.

The form of the curve depends on the salt concentration.

In the absence of external salt,  $T_m$  represents the conformational change (helix  $\rightleftharpoons$  coil transition); the curve is reversible when temperature increases or decreases.

In the presence of KCl when the temperature decreases, gelation and a decrease in  $R$  is observed at a temperature  $T_G < T_m$ . The decrease in the conductivity corresponds to the aggregation of parallel double helices causing the

increase of the effective charge parameter  $\lambda$ . When KCl increases,  $T_G$  goes to  $T_m$  which means that the conformational change coil  $\rightarrow$  helix superposes with the sol  $\rightarrow$  gel transition. The role of external KCl is to screen the electrostatic repulsions between the double helices to allow aggregation i.e. gelation.

The range of external salt concentration ( $C_s$ ), for which a gel exists in the range of temperature explored, strongly depends on the counterions (Fig. 6). The range of  $C_s$  for which  $T_G \neq T_m$  on a 10g/l gellan solution in the given cationic form is given in Table 3.

Thus, in the helical conformation, an ionic selectivity exists:  $\text{TMA} < \text{Li} < \text{Na} < \text{K}$ , corresponding to the order of ability of cations to promote gelation.

These two stages for gelation were also demonstrated by optical rotation or viscosity (see Figs 2 and 5 in Milas *et al.*, 1990).

### GELATION IN THE PRESENCE OF MONOVALENT-DIVALENT COUNTERIONS

When divalent electrolyte  $\text{CaCl}_2$  or  $\text{MgCl}_2$  are progressively added to a Na-gellan solution then the ratio  $R$  varies in a way dependent upon the ratio  $\text{Mg}/\text{Na}$  or  $\text{Ca}/\text{Na}$ . Data concerning the addition of  $\text{MgCl}_2$  on a 10g/l gellan solution in the Na form, are given in Fig. 8. It comes that for:

$$a: 0 \leq [\text{Mg}^{+2}]/[\text{Na}^+] \leq 0.011 \quad \text{Mg}^{+2} \leq 1.6 \times 10^{-4} \text{ N}$$

the variation of  $R$  is that observed with monovalent counterions.  $T_G$  is not observed just  $T_m$ . These curves are reversible in temperature. A decrease in  $R$  when the temperature is lower than  $T_m$  characterizes the behavior in the presence of divalent counterions (Milas *et al.*, 1990) for:

$$b: 0.011 < [\text{Mg}^{+2}]/[\text{Na}^+] \leq 0.12$$

$$1.6 \times 10^{-4} \leq \text{Mg}^{+2} \leq 1.7 \times 10^{-3} \text{ N}$$

A mechanism of aggregation of helices is also observed at  $T_{G1}$  with  $T_{G1} < T_m$ , with a strong decrease in  $R$  corresponding, must probably, to the presence of the monovalent counterions; this transition is reversible.

Finally, the conditions:

$$c: 0.14 \leq [\text{Mg}^{+2}]/[\text{Na}^+]$$

give on cooling an initial sharp decrease in  $R$  corresponding to  $T_{G2} = T_m$  ( $T_{G2}$  corresponds to the gelation temperature imposed by divalent counterions) and the appearance of a large hysteresis between heating and cooling curves (Fig. 9). This hysteresis indicates a

**Table 3.** Range of salt concentration for which  $T_G \neq T_m$  in a 10g/l X-gellan solution in the presence of XCl salt

$X^+$	$K^+$	$Na^+$	$Li^+$	$TMA^+$
XCl (M)	$5 \times 10^{-4} < C_s < 8 \times 10^{-3}$	$10^{-2} < C_s < 5 \times 10^{-2}$	$4 \times 10^{-2} < C_s < 10^{-1}$	absence of $T_G$

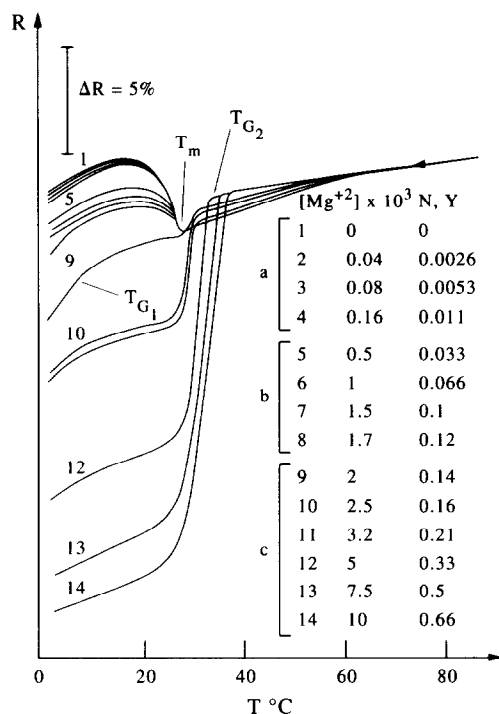


Fig. 8. Evolution of the specific conductivity of Na-gellan solution (10g/l) (expressed by the ratio  $R$ ) with temperature (decreasing temperature). The curves 1 to 14 are obtained for different additions of  $MgCl_2$ .

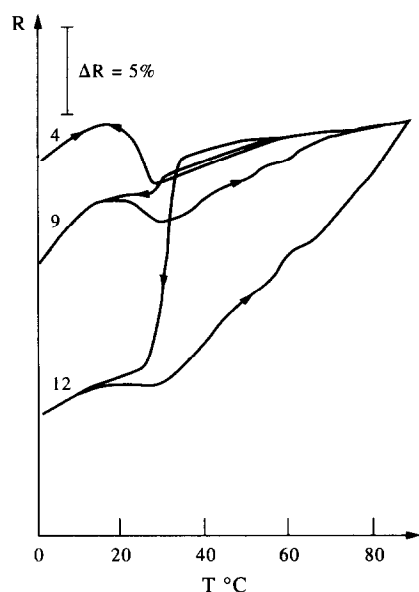


Fig. 9. Hysteresis observed in the presence of  $MgCl_2$  added in a Na-gellan solution (10g/l).  $R$  is related to the specific conductivity of the solution. The solution is prepared at 90°C and firstly cooled. (4) (9) and (12) correspond to the conditions given in Figure 8.

progressive melting of the 3D network i.e. existence of different energies for the helix packing. In this domain  $T_m$  observed on the cooling curve increases due to fixation of divalent counterions.

At lower temperature, break in  $R$  values indicated by

$T_{G1}$  is related to gelation corresponding to the monovalent counterion process and  $T_{G1}$  progressively disappears when the divalent content increases.

## GEL PROPERTIES

Firstly, it was demonstrated that the conditions under which the gel forms are important in controlling the mechanical properties, and elastic modulus. When the gel is progressively cooled (15°C/h)  $E$  is larger ( $9.2 \times 10^4$  Pa) than when the polymer is quenched at 4°C ( $8.5 \times 10^4$  Pa). This demonstrates that the kinetics of aggregation (or phase separation) are very important. Equilibrium of the gel is required before the results discussed in the following are obtained:

A) in the monovalent counterion form. As a first step, the purification was shown to be important. The mechanical properties of the commercial sample are dependent on the presence of divalent counterions (Figs 10 and 11).

On pure samples isolated under different ionic forms, the properties were shown to depend on the counterions; the experimental values are given in Table 4. A strong ionic selectivity exists in the gel phase corresponding to  $Li^+ < Na^+ < K^+$ , which is the same order as that which induces aggregation of double helices.

The elastic modulus depends on the polymer concentration following the relation:

$$E = kC^n$$

The exponent  $n$  is nearly equal to 2, as is usually found (Rinaudo, 1993). Figure 12, shows the physical properties as a function of the salt concentration. Corresponding to the mechanical characteristic curves ( $\sigma(\epsilon)$ ) and fracture facies (Fig. 13), one proposes to identify 3

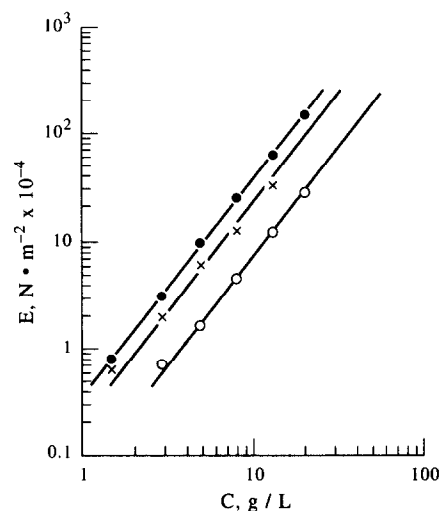
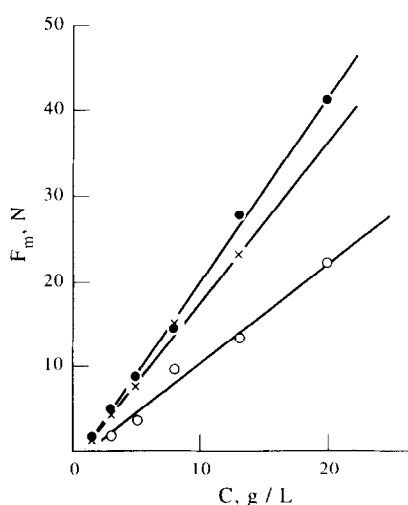
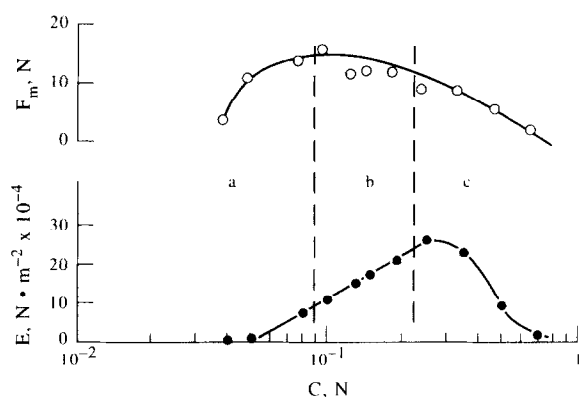


Fig. 10. Elastic modulus  $E$  determined by compression as a function of polymer concentration in log-log plot at constant ionic concentration (0.1 N); ● commercial K-gellan in KCl; X K-gellan purified in KCl; ○ Na-gellan in NaCl.

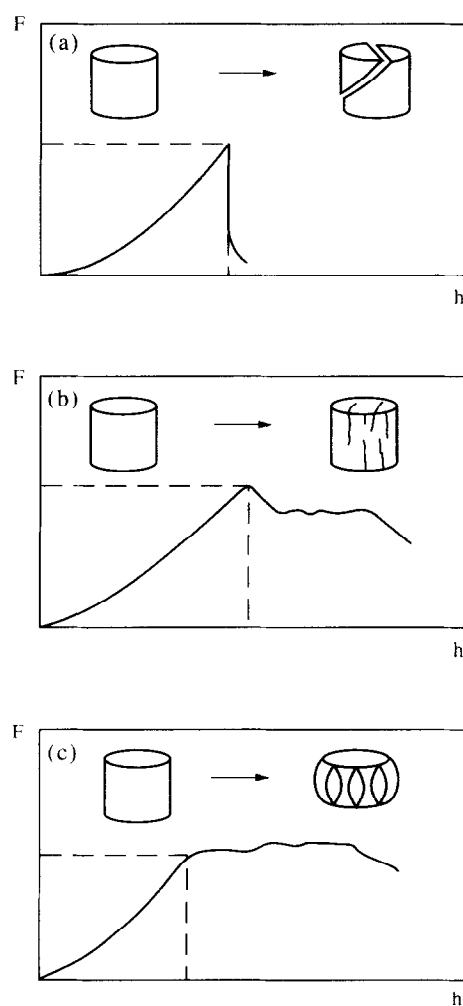
**Table 4.** Elastic modulus,  $E \times 10^{-4}(\text{Pa})$ , and breaking force,  $F_m(\text{N})$ , of X-gellan gels at different polymer concentrations  $C$ , in the presence of 0.1M of different monovalent salts XCl

$C_{\text{g}}/\text{l}$	1.5		3		5		8		13	
	$E$	$F_m$	$E$	$F_m$	$E$	$F_m$	$E$	$F_m$	$E$	$F_m$
KCl	0.63	1.29	1.94	4.17	5.77	7.54	11.7	14.8	31.4	23.10
NaCl			0.7	1.79	1.63	3.51	4.43	9.69	11.9	13.3
LiCl									0.44	

**Fig. 11.** Breaking force ( $F_m$ ) obtained under the conditions given in Fig. 10.**Fig. 12.** Mechanical characteristics of the gels ( $E$ ,  $F_m$ ) obtained as a function of KCl concentration, ( $C$  in mol/l); K-gellan 8g/l  $T = 25^\circ\text{C}$ . a, b, c, refer to the behavior described in Fig. 13.

types of gel behavior. Type (a) gives rise to sharp breaks corresponding to a fragile gel; type (b) and more for (c), corresponds to an increase in the stiffness of the gel with small fractures formed during the break and rugosity of the facies just as corresponding a lower solubility of the polymer and presence of defects. The types a, b, c apply also to the three conditions discussed previously in the presence of divalent counterions (Fig. 8).

**B) in monovalent-divalent counterion form.** As indicated previously,  $\text{Mg}^{+2}$  favours gelation. The maximum

**Fig. 13.** Schematic representation of the three types of gel behavior obtained in presence of salt excess.

of the elastic modulus and breaking force can be compared for  $\text{K}^+$  gels and gels obtained when  $\text{MgCl}_2$  is added in a Na-gellan solution (gellan concentration = 3g/l):

$$E(\text{KCl } 0.3 \text{ N}) = 4.5 \times 10^4 \text{ Pa}$$

$$F_{\text{max}} = 4.17 \text{ N}$$

$$E(\text{MgCl}_2 \text{ } 0.018 \text{ N}) = 6.5 \times 10^4 \text{ Pa}$$

$$F_{\text{max}} = 6.3 \text{ N}$$

These values show that in the presence of  $\text{Mg}^{2+}$  stronger gels are formed as a result of the decrease in the net

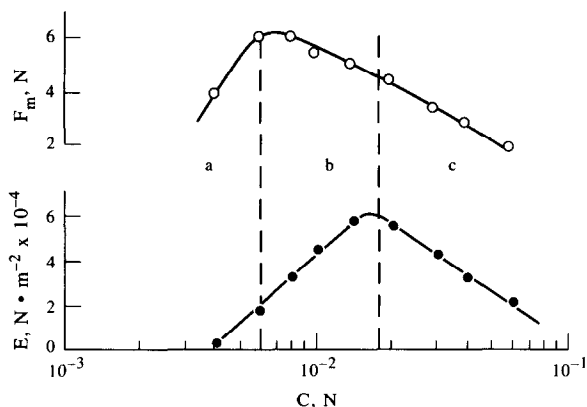


**Fig. 14.** Mechanical characteristics of the gels ( $E$ ,  $F_m$ ) obtained as a function of  $\text{MgCl}_2$  concentration; Na-gellan 3g/l.  $T = 25^\circ\text{C}$ . a, b, c, refer to the behavior described in Fig. 13.

charge of the double helices and stronger association. From optical properties, it seems that even if it is stronger, the association in the presence of divalent counterions implies a lower degree of packing of the double helices.

The physical properties of the gels formed in presence of  $\text{Mg}^{+2}$  are given in Fig. 14; the behavior can be compared with that observed with monovalent counterions (Fig. 12) but the maximum of elastic modulus is obtained for much lower ionic concentration. The gel is formed with a modulus  $E$ , which increases when the ratio  $\text{Mg}/\text{Na}$  increases up to  $\sim([\text{Mg}^{+2}]/[\text{Na}^+]) \sim 0.018$  N) followed by a decrease in the mechanical properties, which is assumed to look like a salting out of the gellan. Progressive fixation of  $\text{Mg}^{+2}$  decreases the net charge and favours the interaction of double helices under limited conditions.

In Fig. 15, the mechanical properties are plotted as a function of  $Y$ , the ratio between  $\text{Mg}^{+2}$  and  $\text{Na}^+$  concentration (expressed in equiv.  $l^{-1}$ ) but at a constant ionic concentration (0.1 N). The three domains correspond approximately to that described by conductivity (Fig. 8). In the first zone, the gel has the properties of that obtained with monovalent salts (up to  $Y = 0.02$ ) then, the modulus increases due to the presence of bivalent counterions up to a ratio  $\text{Mg}^{2+}/\text{Na}^+ \sim 0.2$ . The maximum in the modulus corresponds to that obtained in Fig. 14 (in the absence of a large salt excess). In addition, it was demonstrated that the 3 domains limited by  $Y = 0.02$  and  $0.2$  are independent of the polymer concentration in the range 3 to 20g/l (Fig. 16). Then, only the ionic distribution on the polymer influences the gel structure.

To summarize our results, the characteristic temperatures for gelation on decreasing temperature ( $T_G$ ) and for melting of the gel on increasing temperature ( $T_F$ ) are given in Fig. 17 for a constant ionic concentration.

When  $Y$  is low,  $T_G$  and  $T_F$  vary slowly and are very near the values obtained with the monovalent counter-

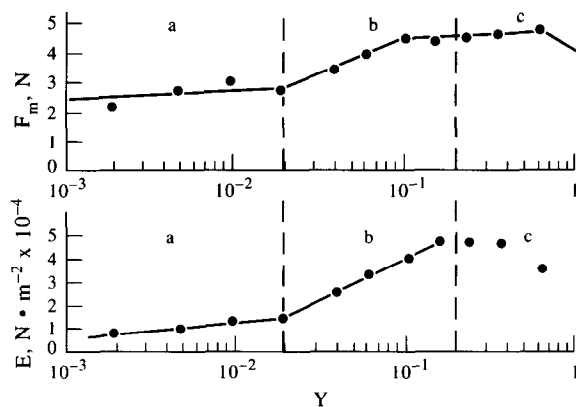


**Fig. 15.** Mechanical characteristics of the gels ( $E$ ,  $F_m$ ) obtained for different ratios  $Y = [\text{Mg}^{2+}]/[\text{Na}^+]$  and constant ionic concentration (0.1 N); Na-gellan 3g/l,  $T = 25^\circ\text{C}$ . a, b, c, refer to the behaviour described in Figs 8 and 13.

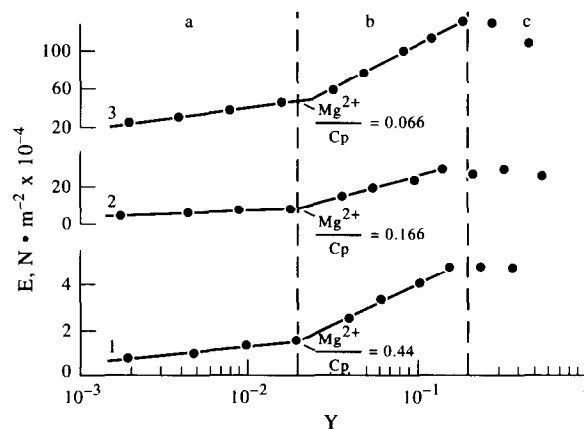


**Fig. 16.** Elastic modulus of the gels obtained for different ratios  $Y = (\text{Mg}^{2+})/[\text{Na}^+]$  and different polymer concentrations at constant ionic concentration (0.1 N). a, b, c refer to the behavior described in Figs 8 and 13. (a) 1: Na-gellan 3g/2; Na-gellan 8g/3; Na-gellan 20g/l

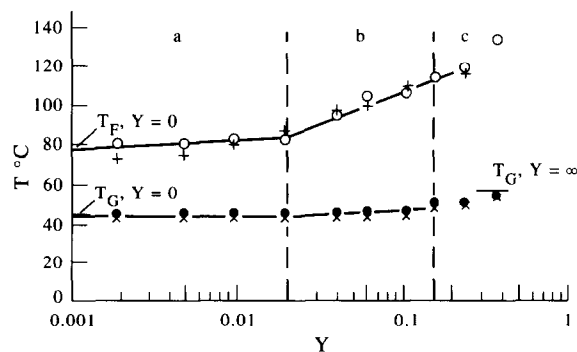


**Fig. 17.** Influence of the ratio  $Y$  on the gelling temperature ( $T_G$ ) and melting temperature ( $T_F$ ) for K- or Na-gellan (3g/l) at constant ionic concentration ( $[\text{Na}^+]$  or  $[\text{K}^+] + [\text{Mg}^{2+}] = 0.1$  N).  $T = 25^\circ\text{C}$ ; a, b, c refer to the behaviour described in figures 8 and 13. X  $T_G$ , +  $T_F$  Na-gellan; ●  $T_G$  OTF K-gellan.

ion ( $K^+$  or  $Na^+$  form) ( $Y = 0$ ). When  $Mg^{+2}$  is increasing, in the second domain, the role of divalent counterions becomes important, and the hysteresis between heating and cooling curves increases compared with monovalent counterions, corresponding to the larger stability of the helices and of the aggregates in the presence of divalent counterions.

## CONCLUSION

This paper describes the mechanism of gelation of gellan in the presence of monovalent counterions or for progressive addition of divalent counterions. First, in dilute solution, under monovalent ionic form, a reversible conformational transition exists with no ionic selectivity; in the divalent salt form, the gellan transition shows an hysteresis even in very dilute solution (0.5g/l) in relation to its ability to form aggregates.

At higher concentrations, in the presence of external monovalent electrolytes, a sol-gel transition is promoted with an ionic selectivity; it is interpreted as a progressive aggregation of double helices in the order  $TMA < Li < Na < K$ . In some respects, the mechanisms are similar to that proposed for gelation of K-carrageenans in relation to the ionic selectivity. Melting of the gel is also a multistep process.

Progressive addition of divalent counterions promotes gelation for much lower concentrations than in monovalent counterions. Also, the maximum in elastic modulus is larger with divalent counterions.

In the presence of divalent counterions controlled by the ratio  $Y = C^{2+}/C^{1+}$  at constant ionic concentration (0.1 N) gelation is observed for low  $Y$  values. The gels obtained have a higher elastic modulus and larger thermal stability.

Depending on the salt concentration, the mechanical behavior is described by three typical strain stress curves for monovalent and divalent counterions. The same

mechanism of gelation is then suggested for the two types of counterions, the counterion interacting more with gellan giving the more stable gel; the mechanism involves aggregation of stiff double helices forming domains which then connect.

The mechanism also implies an important kinetic process which causes variability in the properties of gel obtained depending on the experimental conditions adopted.

## REFERENCES

- Chandrasekaran, R., Puigjaner, L.C., Jayce, K.L. & Arnott, S. (1988). Cation interactions in gellan: an X-ray study of the potassium salt. *Carbohydr. Res.*, **181**, 23–40.
- Chandrasekaran, R. & Thailambal, V.G. (1990). The influence of calcium ions, acetate and L-glycerate groups on the gellan double helix. *Carbohydr. Polym.*, **12**, 431–442.
- Crescenzi, V., Dentini, M. & Dea, I.C.M. (1987). The influence of side chains on the dilute solution properties of three structurally related bacterial anionic polysaccharides. *Carbohydr. Res.*, **160**, 283–302.
- Grasdalen, H. & Smidsrod, O. (1987). Gelation of gellan gum. *Carbohydr. Polym.*, **7**, 371–393.
- Jansson, P.E., Lindberg, B. & Sandford, P.A. (1983). Structural studies of gellan gum, an extracellular polysaccharide elaborated by *Pseudomonas elodea*. *Carbohydr. Res.*, **124**, 135–139.
- Milas, M., Shi, X. & Rinaudo, M. (1990). On the physicochemical properties of gellan gum. *Biopolymers*, **30**, 451–464.
- Rinaudo, M., Rochas, C. & Michels, B. (1983). Etude par absorption ultrasonore de la fixation sélective du potassium sur le K-carraghénane. *J. Chim. Phys.*, **80**, 305–308.
- Rinaudo, M. (1993). Gelation of polysaccharides. *J. Intell. Mater. Sys. Struct.*, **4**, 210–215.
- Robinson, G., Manning, C.E., Morris, E.R. & Dea, I.C.M. (1988). Side-chain main-chain interactions in bacterial polysaccharides. In *Gums and Stabilizers for the Food in Industry 4*, eds G.O. Phillips, D.J. Wedlock & P.A. Williams. IRL Press Oxford, pp.173–181.
- Shi, X. (1990). Relation entre la conformation et les propriétés d'un polysaccharide bactérien, le gellane, Thesis Grenoble, France.